



Molecular Physics

An International Journal at the Interface Between Chemistry and Physics

ISSN: 0026-8976 (Print) 1362-3028 (Online) Journal homepage: <https://www.tandfonline.com/loi/tmph20>

Hartree-Fock instabilities and the diagonal Born-Oppenheimer correction

James H. Thorpe & John F. Stanton

To cite this article: James H. Thorpe & John F. Stanton (2020): Hartree-Fock instabilities and the diagonal Born-Oppenheimer correction, Molecular Physics, DOI: [10.1080/00268976.2020.1742936](https://doi.org/10.1080/00268976.2020.1742936)

To link to this article: <https://doi.org/10.1080/00268976.2020.1742936>



Published online: 22 Apr 2020.



Submit your article to this journal [↗](#)



Article views: 77





View related articles [↗](#)



View Crossmark data [↗](#)

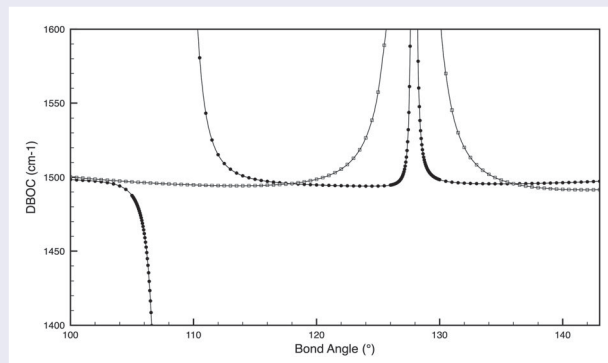
Hartree-Fock instabilities and the diagonal Born-Oppenheimer correction

James H. Thorpe  and John F. Stanton 

The Quantum Theory Project, Department of Chemistry, The University of Florida, Gainesville, FL, USA

ABSTRACT

The NO and NO₂ radicals are used to demonstrate how instabilities in Hartree-Fock wavefunctions can result in unsatisfactory, or even unphysical, values of the diagonal Born-Oppenheimer correction (DBOC). For NO, an avoided crossing between two UHF solutions of ²Π symmetry results in a nearly 1 kJ/mol (80 cm⁻¹) defect in the SCF-level DBOC just beyond the equilibrium bond distance. In that case, CCSD is able to recover essentially correct behaviour. For ground-state (\tilde{X}^2A_1) NO₂, a second-order CPHF pole is observed in the dependence of the DBOC on the bending angle at a geometry rather far from the true conical intersection between the \tilde{X}^2A_1 and \tilde{A}^2B_2 states, an artifact that cannot be completely ameliorated by any method short of full CI. These effects arise from well-known problems associated with (near) instabilities of Hartree-Fock solutions, though there is little in the literature about this in the current context. The goal of this paper is to raise awareness of these potential problems, as the DBOC (adiabatic correction) is now an essential part of many modern protocols for high-accuracy calculations, and to provide some comments of the causes of these phenomena.



ARTICLE HISTORY

Received 31 December 2019
Accepted 9 March 2020

KEYWORDS

Quantum chemistry;
diagonal born-oppenheimer
correction; nonadiabatic
behavior; thermochemistry

1. Introduction

For the majority of chemical applications, *ab initio* calculations are performed within the framework of the Born-Oppenheimer approximation (BOA) [1], where the electronic Schrödinger equation is solved with the assumption that contributions from the nuclear kinetic energy operator can be safely ignored. It is this process that permits the construction of molecular potential energy surfaces (that are identical for all isotopologues). The BOA is both computationally and conceptually straightforward, and provides the foundation upon which many of our qualitative models of chemistry are built.

However, when high accuracy is called for, it is fairly common to include the first-order correction to the electronic energy due to the nuclear kinetic energy operator, even when interactions with other electronic states (non-adiabatic effects) are unimportant. This contribution is known as the diagonal Born-Oppenheimer correction (DBOC), or sometimes the ‘adiabatic correction’. Addition of the DBOC to the usual electronic energy produces potential energy surfaces that are still well-defined, but are now mass- (isotope-) dependent. The DBOC is one of a handful of small corrections that are sometimes included when very high accuracy is sought. This is particularly important for hydrogen-containing

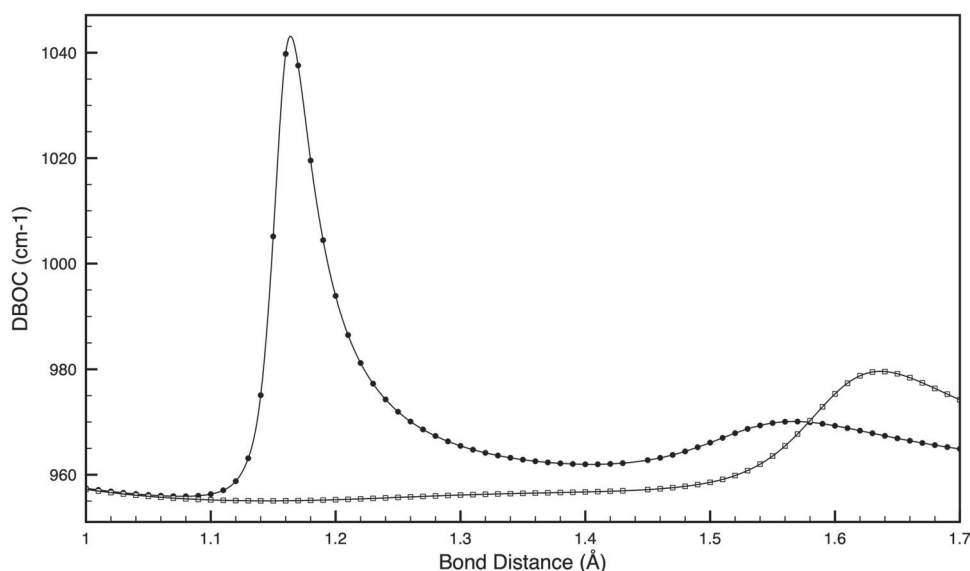


Figure 1. Plot of the UHF (filled circles) and ROHF (unfilled squares) level DBOC as a function of bond distance for ${}^2\Pi$ NO with the aug-cc-pVTZ basis set. Solid points are ‘real’ data, while curves are obtained via cubic spline interpolation. The UHF DBOC rapidly swells just beyond the equilibrium bond distance of roughly 1.15 \AA , a result of near instabilities in the wavefunction.

molecules, where the effects of the DBOC are generally more pronounced.

For example, the (small) electric dipole moment of the HD molecule can be attributed to contributions from the DBOC [2], rather than to more complicated non-adiabatic interactions with excited electronic states. In addition, the DBOC is commonly employed in rigorous treatments of potential energy surfaces [2–16], and is widely used as an ingredient in high-accuracy recipes for thermochemical calculations [17–28].

Particularly in the world of high-accuracy thermochemistry, the DBOC is most commonly evaluated using SCF wavefunctions [17–31], though it has been implemented at coupled-cluster and other correlated levels of theory [32–35]. The computational cost of evaluating the DBOC is comparable to that of an analytic second derivative (Hessian) calculation, so evaluation of this quantity at correlated levels is correspondingly complicated, somewhat uncommon, and expensive. While the dipole moment of HD referenced above was done with CISD (which is exact for two electrons), the SCF-level DBOC is typically employed as a (small) correction when other properties of molecules, such as bond energies or force constants, have otherwise been evaluated with great care using various high-level techniques and methods.

The purpose of this (short) paper is to demonstrate that the DBOC should perhaps be monitored with care, especially when calculated at the SCF level of theory. Since it is formally a second-order property, and therefore depends upon the response of the wavefunction to an external perturbation, and, consequently, the treatment

of ‘excited states’ (in the sense of standard first-order perturbation theory), one can expect relatively large diagonal Born-Oppenheimer corrections when there is efficient coupling with low-lying electronic states [36]. However, as has been amply documented and demonstrated [37–42], the ‘excitation energies’ associated with the SCF wavefunction response (the eigenvalues of the associated orbital rotation stability matrix [43–47]) are frequently poor approximations of the true values. Thus, (near) instabilities of the SCF solutions can result in divergent response of the wavefunction, and with it, the DBOC. It is important to recognise that this can occur in regions of the potential energy surface that contain no such features at the full CI limit.

These curious effects have previously been studied in some detail [37, 40, 41] for other properties depending on wavefunction response, such as force constants, electric polarisabilities, etc., but, to the best of our knowledge, the fact that the DBOC is susceptible to similar issues has only been mentioned once before in the literature [6]. To this end, the following sections will use the NO and NO₂ radicals to illustrate some qualitative features of problems associated with the DBOC, and to recommend a few tests that can be made when the adiabatic correction displays troublesome behaviour in numerical work.

2. The DBOC

The energy correction known as the DBOC is given by

$$\Delta E_{DBOC} = \langle \Psi(r; R) | \hat{T}_N(R) | \Psi(r; R) \rangle \quad (1)$$

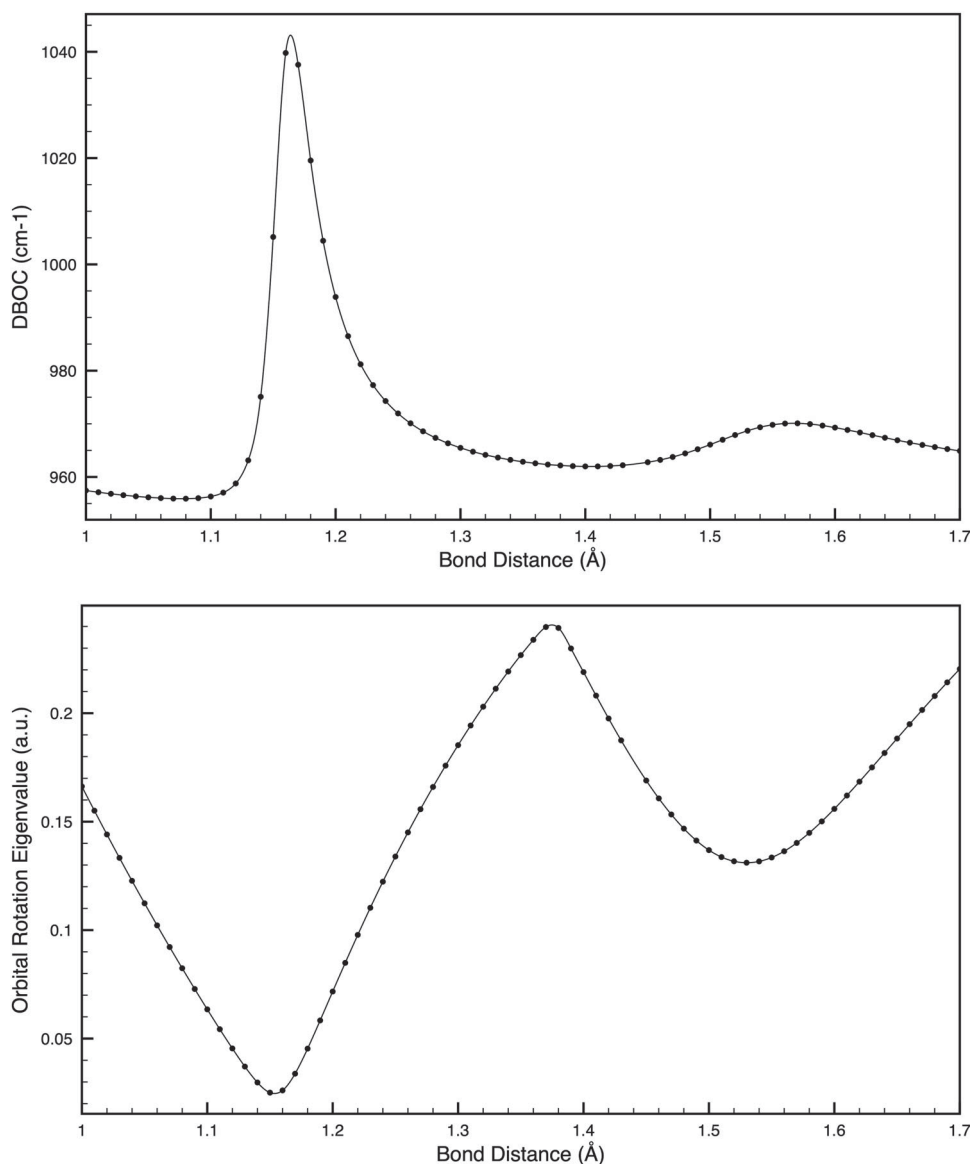


Figure 2. Plot of the DBOC (top) and the totally symmetric orbital rotation eigenvalue (bottom) for ${}^2\Pi$ NO as a function of bond distance. Values are calculated with UHF/aug-cc-pVTZ. Solid points are ‘real’ data, while curves are obtained via cubic spline interpolation. The near-zero orbital rotation eigenvalue is a result of an avoided crossing with an alternate SCF solution, and results in an artifact in the UHF-level DBOC.

where Ψ is the normalised Born-Oppenheimer electronic wavefunction and \hat{T}_N is the nuclear kinetic energy operator. The pioneering work of Sellers and Pulay [29, 30] demonstrated that the SCF-level DBOC can be calculated using only first derivatives of the wavefunction [48]. The later efforts of Handy *et al.* [31] demonstrated how to efficiently and analytically compute this correction by employing the CPHF equations of Gerratt and Mills [49].

As has already been mentioned, these CPHF solutions are sensitive to instabilities in the SCF wavefunction, and become singular when there is a zero eigenvalue of the orbital rotation stability matrix (when the RPA excitation energy is zero). One of the terms in the SCF-level

DBOC equations depends upon the square of the CPHF coefficients, and results in a positive, second-order pole structure of the DBOC near a CPHF singularity, regardless of whether the nearby ‘state’ is higher or lower in energy (that is, unphysically large and positive values are obtained whether the solution is ‘barely stable’ or ‘barely unstable’).

3. NO

The NO radical is an illustrative (and cautionary) example of SCF-level DBOC instabilities, and it is this species that first brought these potential dangers to the authors’

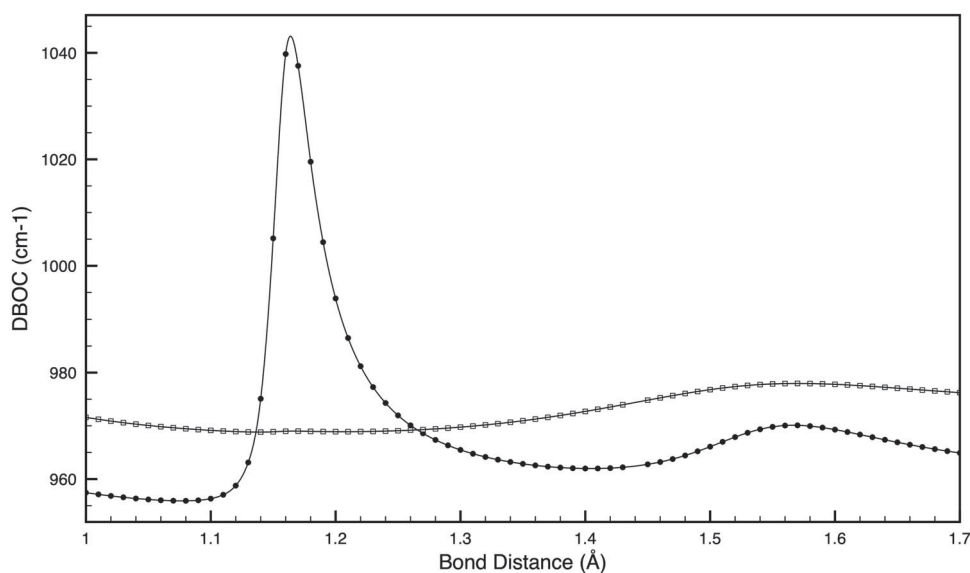


Figure 3. Plot of the DBOC of ${}^2\Pi$ NO as a function of bond distance calculated using UHF (filled circles) and CCSD (unfilled squares) with the aug-cc-pVTZ basis set. Solid points are ‘real’ data, while curves are obtained via cubic spline interpolation. The CCSD DBOC appears to overcome the artifact displayed by its UHF reference wavefunction.

attention. While modifying the HEAT model chemistry [20], it was observed that ROHF and UHF DBOCs for the $\tilde{X}^2\Pi$ state of this molecule differed by nearly 70 cm^{-1} , a finding briefly commented upon in that work. Further investigation reveals that the UHF DBOC changes rather rapidly at bond lengths just beyond equilibrium, a region where the ROHF DBOC is relatively stable, as shown in Figure 1. In Figure 2, the UHF level DBOC and the lowest totally symmetric orbital rotation eigenvalue are plotted as a function of interatomic distance. At a bond length of roughly 1.15 \AA , there is a local minimum of this orbital rotation eigenvalue in a region where CPHF reveals an avoided crossing between two SCF solutions. While the orbital rotation eigenvalue never reaches zero, the influence of the nearby SCF solution is enough to cause a nearly 1 kJ/mol artifact in the SCF-level DBOC. While this might seem like a small contribution to the energy, it is certainly relevant in the domain of high-accuracy computational thermochemistry.

In this case, where the orbital rotation eigenvalue is simply varying rapidly, rather than leading to a singularity in the CPHF equations, the behaviour of the DBOC can largely be remedied using CC wavefunctions. Figure 3 plots the SCF and CCSD level DBOC of NO as a function of bond distance: the nearly 80 cm^{-1} anomaly that plagues the UHF DBOC essentially disappears with CCSD. That there is no significant fluctuation in the CCSD DBOC clearly indicates that the behaviour of the Hartree-Fock level correction here is entirely unphysical, and is a testament to the ability of coupled-cluster

theory to correct for moderate deficiencies in reference wavefunctions [50].

The example of the NO radical should be regarded as somewhat of a warning to computational chemists who regularly employ the Hartree-Fock level DBOC in their high-accuracy protocols. For open-shell molecules, SCF wavefunctions (both UHF and ROHF) are prone to issues of the kind displayed by NO, and erroneously large diagonal Born-Oppenheimer corrections could easily escape the attention of the practicing computational chemist.

4. NO₂

The NO₂ radical provides another example of issues encountered with the SCF-level DBOC. Figure 4 shows the DBOC for the 2A_1 state and the orbital rotation eigenvalue that serves to connect the 2A_1 and 2B_2 solutions at the UHF/cc-pVDZ level of theory as a function of ONO bond angle. At a bond angle of roughly 128° , this orbital rotation eigenvalue passes through zero (that is, at smaller angles, the 2A_1 SCF solution is unstable with respect to a symmetry-broken solution). As a consequence, properties that depend on derivatives of the wavefunction, the DBOC included, become singular at this threshold angle.

Figure 5 plots the SCF and CCSD level DBOC as a function of bond angle. Unlike NO, CCSD for NO₂ does not resolve the singularity at 128° arising from divergence of the CPHF equations (it is now truly a CPHF pole of the kind referenced in [37, 41]), though it goes a long

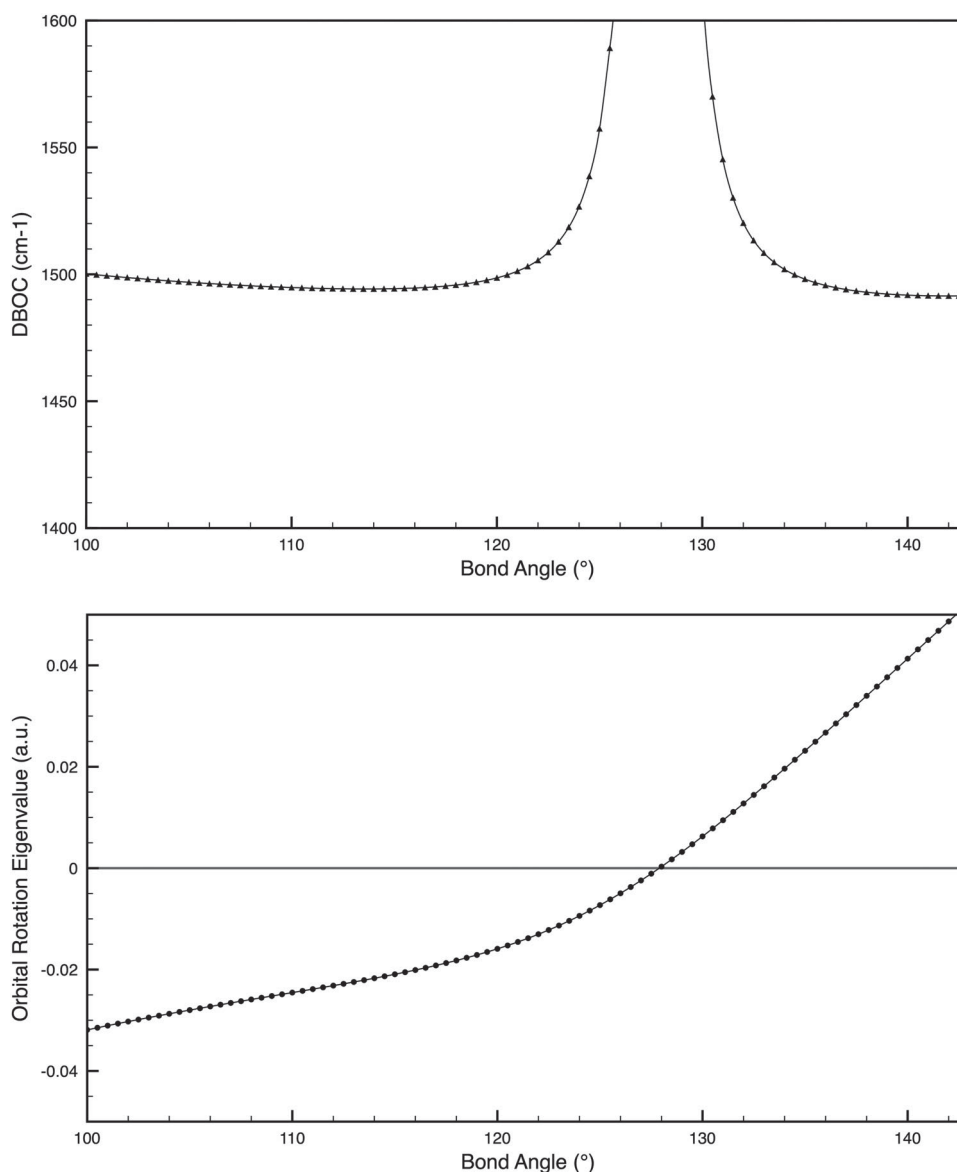


Figure 4. Plot of the UHF/cc-pVDZ DBOC (top) and orbital rotation eigenvalue of b_2 symmetry (bottom) for the 2A_1 state of NO_2 as a function of ONO bond angle, with fixed bond lengths of 1.27 \AA . Solid points are ‘real’ data, while curves are obtained via cubic spline interpolation. The orbital rotation eigenvalue, which connects the 2A_1 and 2B_2 states, passes through zero at a bond angle of roughly 128° , resulting in a divergence of the response of the SCF wavefunction.

way toward reducing the width of this diabolical feature. It should be emphasised that the pole here is unphysical – the true crossing point of the 2A_1 and 2B_2 states occurs at a bond angle below 110° , to which the SCF-DBOC is oblivious. That the response of the SCF wavefunction cannot satisfactorily account for the approach of these two states speaks to its inability to represent behaviour associated with vibronic (Herzberg-Teller) coupling with even a semblance of fidelity. It is possible that an orbital-unrelaxed approach to the CCSD level DBOC, where the response of the reference wavefunction orbitals is excluded, could overcome these CPHF-poles.

We are currently considering such a development in our lab.

CCSD, on the other hand, predicts a correlation pole at the crossing point of the CCSD 2A_1 and EOMEE-CCSD 2B_2 potential energy surfaces (of the type discussed in Ref. [41]), which is indeed in the region of the true singularity. However, it exhibits a complicated pole structure, which leads in one limit to a negative (and therefore clearly wrong) value of the DBOC. This point is discussed in the [appendix](#), where it is shown that the pole becomes second-order in the full CI limit (as it must be), but its behaviour here is compromised

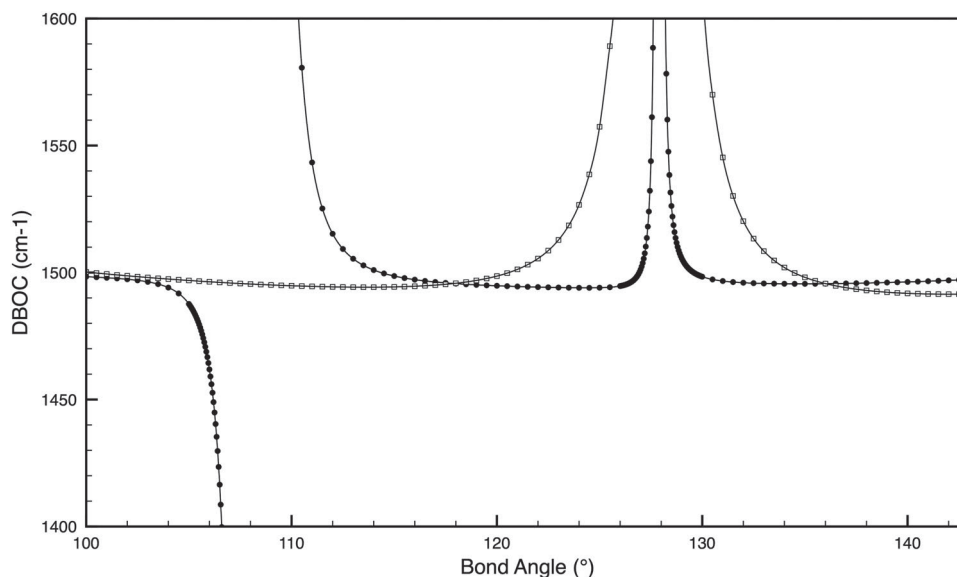


Figure 5. Plot of the UHF (unfilled squares) and CCSD (filled circles) DBOCs for the 2A_1 state of NO_2 calculated with the cc-pVDZ basis set as a function of ONO bond angle at a fixed bond length of 1.27 Å. Solid points are 'real' data, while curves are obtained via cubic spline interpolation. The CPHF pole of the DBOC at 128° is a consequence of instability of the Hartree-Fock wavefunction. The correlation pole at roughly 108° is centred around the crossing point of the CCSD 2A_1 and EOMEE-CCSD 2B_2 potential energy surfaces. Off the scale of the graph is a region (just below a bond angle of 108°) at which the CCSD DBOC attains unphysical, *negative* values.

by the incomplete treatment of electron correlation in CCSD.

5. Diagnostics

Following the analysis above, a few methods can be recommended to diagnose potentially problematic DBOCs. The first, and most reliable, has been employed through the majority of this paper: the eigenvalues of the orbital rotation stability matrix. It should be pointed out that negative eigenvalues (which indicate a lower-lying SCF solution) in-and-of themselves are not predictors of poor SCF behaviour. Rather, only the magnitude of the eigenvalue should be considered: values near zero can potentially give rise to the CPHF poles discussed above. It is difficult to say exactly when a nearby SCF solution will cause problems, but in the case of NO, an orbital rotation eigenvalue of 0.03 a.u. was sufficient to cause a nearly 1 kJ/mol error in the SCF DBOC.

The second check for potential issues has also been mentioned already: disagreement between DBOC energies calculated with UHF and ROHF wavefunctions. In a well behaved system, the value of the DBOC should not vary much between these two levels of theory. As these treatments tend to (though by no means always) encounter instabilities in different regions of potential energy surfaces, significant differences between their DBOCs could indicate that at least one of them is problematic [51].

Last, in the case of high-accuracy calculations on molecules that are well-represented by the adiabatic approximation, the DBOC contribution to quantities such as total atomisation energies and enthalpies of formation should be small [52]. If this is not the case, it is quite possible that the SCF solutions are near a point of instability, and the orbital rotation eigenvalues should be checked. If neither SCF solution is near a point of instability, then it is worthwhile to do a (more expensive) correlated calculation. If the large DBOC persists, then it is likely that there is a true nearby and strongly coupled state, and it might be that the adiabatic approximation is inappropriate. In such situations, the DBOC should be abandoned and a multistate treatment may be in order.

6. Summary

In the majority of quantum chemical calculations, the electronic wavefunction is calculated within the clamped nucleus approximation. The resulting Born-Oppenheimer electronic energy is missing a contribution from the nuclear kinetic energy. In high-accuracy work, quantum chemists account for this typically small, but sometimes important, contribution via the diagonal Born-Oppenheimer correction, usually at the SCF level of theory. In this work, we have given two examples where the Hartree-Fock level DBOC yields unsatisfactory, or even unphysical, results. As the DBOC depends upon the response of the wavefunction (in a manner similar to

force constants), it is sensitive to instabilities of the SCF solutions; zero eigenvalues of the orbital rotation stability matrix result in divergent CPHF solutions and DBOC energies. In the case of NO, an avoided crossing of two SCF solutions results in a nearly 1 kJ/mol artifact in the DBOC near the equilibrium bond distance, which could largely be mended using CCSD theory. However, for NO₂, nearby SCF states result in singular CPHF solutions and a second-order CPHF pole that cannot be remedied with a CCSD wavefunction. These results indicate that the DBOC, though usually only a small contribution to molecular properties, should be considered in high-accuracy work with the same degree of caution as force constants, which are well understood to be potentially problematic, especially in open-shell systems [53]. Last, we suggested a few simple tests, namely careful observation of the orbital rotation eigenvalues and chemical intuition, to help diagnose potentially flawed DBOCs.

Acknowledgements

This paper is dedicated to honouring the 60th birthday of Jürgen Gauss, whose mastery of coupled-cluster gradient theory has benefited us all, as well as the memory of Werner Kutzelnigg.

Disclosure statement

No potential conflict of interest was reported by the author(s).

Funding

The authors of this paper were funded by the National Science Foundation under Award No. CHE-1664325 and by the Air Force Office of Scientific Research under Award No. FA9550-16-1-0117.

ORCID

James H. Thorpe  <http://orcid.org/0000-0002-9258-006X>

John F. Stanton  <http://orcid.org/0000-0003-2345-9781>

References

- [1] M. Born and R. Oppenheimer, *Ann. Phys.* **389**, 457 (1927).
- [2] S.L. Hobson, E.F. Valeev, A.G. Császár and J.F. Stanton, *Mol. Phys.* **107**, 1153 (2009).
- [3] W. Kołos and L. Wolniewicz, *J. Chem. Phys.* **41**, 3663 (1964).
- [4] W. Kołos and L. Wolniewicz, *J. Chem. Phys.* **43**, 2429 (1965).
- [5] O.L. Polyansky and J. Tennyson, *J. Chem. Phys.* **110**, 5056 (1999).
- [6] J.J. Lutz and J.M. Hutson, *J. Mol. Spectrosc.* **330**, 43 (2016).
- [7] P. Barletta, S.V. Shirin, N.F. Zobov, O.L. Polyansky, J. Tennyson, E.F. Valeev and A.G. Császár, *J. Chem. Phys.* **125**, 204307 (2006).
- [8] C. Fábri, G. Czako, G. Tasi and A.G. Császár, *J. Chem. Phys.* **130**, 134314 (2009).
- [9] G. Tarczay, A.G. Császár, W. Klopper, V. Szalay, W.D. Allen and H.F. Schaefer, *J. Chem. Phys.* **110**, 11971 (1999).
- [10] K. Aarset, A.G. Császár, E.L. Sibert, W.D. Allen, H.F. Schaefer, W. Klopper and J. Noga, *J. Chem. Phys.* **112**, 4053 (2000).
- [11] A.G. Császár, V. Szalay and M.L. Senent, *J. Chem. Phys.* **120**, 1203 (2004).
- [12] G. Tarczay, A.G. Császár, M.L. Leininger and W. Klopper, *Chem. Phys. Lett.* **322**, 119 (2000).
- [13] A. Owens, S.N. Yurchenko, A. Yachmenev, J. Tennyson and W. Thiel, *J. Chem. Phys.* **142**, 244306 (2015).
- [14] M. Pavanello, L. Adamowicz, A. Alijah, N.F. Zobov, I.I. Mizus, O.L. Polyansky, J. Tennyson, T. Szidarovszky and A.G. Császár, *J. Chem. Phys.* **136**, 184303 (2012).
- [15] A. Owens, S.N. Yurchenko, A. Yachmenev, J. Tennyson and W. Thiel, *J. Chem. Phys.* **145**, 104305 (2016).
- [16] X. Huang, D.W. Schwenke and T.J. Lee, *J. Chem. Phys.* **129**, 214304 (2008).
- [17] A. Tajti, P.G. Szalay, A.G. Császár, M. Kállay, J. Gauss, E.F. Valeev, B.A. Flowers, J. Vázquez and J.F. Stanton, *J. Chem. Phys.* **121**, 11599 (2004).
- [18] Y.J. Bomble, J. Vázquez, M. Kállay, C. Michauk, P.G. Szalay, A.G. Császár, J. Gauss and J.F. Stanton, *J. Chem. Phys.* **125**, 064108 (2006).
- [19] M.E. Harding, J. Vázquez, B. Ruscic, A.K. Wilson, J. Gauss and J.F. Stanton, *J. Chem. Phys.* **128**, 114111 (2008).
- [20] J.H. Thorpe, C.A. Lopez, T.L. Nguyen, J.H. Baraban, D.H. Bross, B. Ruscic and J.F. Stanton, *J. Chem. Phys.* **150**, 224102 (2019).
- [21] J.M.L. Martin and G. de Oliveira, *J. Chem. Phys.* **111**, 1843 (1999).
- [22] A.D. Boese, M. Oren, O. Atasoylu, J.M.L. Martin, M. Kállay and J. Gauss, *J. Chem. Phys.* **120**, 4129 (2004).
- [23] A. Karton, E. Rabinovich, J.M.L. Martin and B. Ruscic, *J. Chem. Phys.* **125**, 144108 (2006).
- [24] M.S. Schuurman, S.R. Muir, W.D. Allen and H.F. Schaefer, *J. Chem. Phys.* **120**, 11586 (2004).
- [25] H.M. Jaeger, H.F. Schaefer, J. Demaison, A.G. Császár and W.D. Allen, *J. Chem. Theory. Comput.* **6**, 3066 (2010).
- [26] K.A. Peterson, D. Feller and D.A. Dixon, *Theor. Chem. Acc.* **131**, 1079 (2012).
- [27] A. Karton, *Wiley Interdiscip. Rev. Comput. Mol. Sci.* **6**, 292 (2016).
- [28] S.J. Klippenstein, L.B. Harding and B. Ruscic, *J. Phys. Chem. A* **121**, 6580 (2017).
- [29] H. Sellers and P. Pulay, *Chem. Phys. Lett.* **103**, 463 (1984).
- [30] H. Sellers, *Chem. Phys. Lett.* **108**, 339 (1984).
- [31] N.C. Handy, Y. Yamaguchi and H.F. Schaefer, *J. Chem. Phys.* **84**, 4481 (1986).
- [32] D.W. Schwenke, *J. Phys. Chem. A* **105**, 2352 (2001).
- [33] J. Gauss, A. Tajti, M. Kállay, J.F. Stanton and P.G. Szalay, *J. Chem. Phys.* **125**, 144111 (2006).
- [34] E.F. Valeev and C.D. Sherrill, *J. Chem. Phys.* **118**, 3921 (2003).
- [35] A. Tajti, P.G. Szalay and J. Gauss, *J. Chem. Phys.* **127**, 014102 (2007).
- [36] Of course, when the DBOC becomes too large (in regions sufficiently close to intersections or weakly avoided crossings), the adiabatic approximation must be abandoned.

- [37] T.D. Crawford, J.F. Stanton, W.D. Allen and H.F. Schaefer, *J. Chem. Phys.* **107**, 10626 (1997).
- [38] J.C. Saeh and J.F. Stanton, *J. Chem. Phys.* **111**, 8275 (1999).
- [39] T.D. Crawford, E. Kraka, J.F. Stanton and D. Cremer, *J. Chem. Phys.* **114**, 10638 (2001).
- [40] P.G. Szalay, J. Vázquez, C. Simmons and J.F. Stanton, *J. Chem. Phys.* **121**, 7624 (2004).
- [41] J.F. Stanton, *J. Chem. Phys.* **115**, 10382 (2001).
- [42] J.F. Stanton, *J. Chem. Phys.* **126**, 134309 (2007).
- [43] J. Čížek and J. Paldus, *J. Chem. Phys.* **47**, 3976 (1967).
- [44] J. Paldus and J. Čížek, *Chem. Phys. Lett.* **3**, 1 (1969).
- [45] J. Paldus and J. Čížek, *Phys. Rev. A* **2**, 2268 (1970).
- [46] J. Paldus and J. Čížek, *J. Chem. Phys.* **54**, 2293 (1971).
- [47] J. Paldus and J. Čížek, *Can. J. Chem.* **63**, 1803 (1985).
- [48] Note that the separation of the kinetic energy operator into first derivatives acting upon the left and right hand wavefunctions is a critical step in any numerical implementation of the DBOC, and is of course employed in its derivation and evaluation at correlated levels of theory, see refs. [32–35].
- [49] J. Gerratt and I.M. Mills, *J. Chem. Phys.* **49**, 1719 (1968).
- [50] H. Sekino and R.J. Bartlett, *J. Chem. Phys.* **82**, 4225 (1985).
- [51] It should be noted that the examples given in this work have largely utilized UHF wavefunctions. This is perhaps misleading, as ROHF (and RHF!) are by no means immune from problems regarding orbitals stability. We have employed UHF simply for the reason that the CCSD-level DBOC using ROHF wavefunctions has not been coded in any quantum chemistry package.
- [52] A possible exception to this statement is the case of activation energies. The DBOC is related to the expectation value of the second derivative of the wavefunction with respect to nuclear coordinate. For many transition states, the wavefunction is indeed varying rapidly, and thus “large” contributions of the DBOC to activation energies (over one kJ/mol), are *not necessarily* unexpected. See ref. [20].
- [53] J.F. Stanton and J. Gauss, in *Advances in Chemical Physics* (2003), chap. chapter2, pp. 101–146.
- [54] W. Kutzelnigg, *Mol. Phys.* **90**, 909 (1997).
- [55] L. Adamowicz, W.D. Laidig and R.J. Bartlett, *Int. J. Quantum. Chem.* **26**, 245 (1984).
- [56] H. Koch, H.J.A. Jensen, P. Jørgensen, T. Helgaker, G.E. Scuseria and H.F. Schaefer, *J. Chem. Phys.* **92**, 4924 (1990).

Appendix

A.1 Correlation poles of the DBOC

The DBOC for a molecule consisting of N atoms can be expressed in coupled-cluster theory [33] as

$$\Delta E_{DBOC} = - \sum_{\alpha}^{3N} \left(\frac{1}{2M_{\alpha}} \left\langle \tilde{\Psi}_{CC} \left| \frac{\partial^2}{\partial \alpha^2} \right| \Psi_{CC} \right\rangle + N_{RR} \right), \quad (\text{A1})$$

or, equivalently,

$$\Delta E_{DBOC} = \sum_{\alpha}^{3N} \left(\frac{1}{2M_{\alpha}} \left\langle \frac{\partial}{\partial \alpha} \tilde{\Psi}_{CC} \left| \frac{\partial}{\partial \alpha} \Psi_{CC} \right\rangle + N_{LR} \right). \quad (\text{A2})$$

Here α runs over all Cartesian coordinates associated with nuclei of mass M_{α} , and N_{RR} and N_{LR} are normalisation factors that come from the requirement that the wavefunction be

normalised in order to exploit the treatment of the DBOC put forward by Kutzelnigg [54]. The $\langle \tilde{\Psi}_{CC} |$ and $|\Psi_{CC}\rangle$ are the left- and right-hand CC wavefunctions respectively, and are given by

$$\langle \tilde{\Psi}_{CC} | = \langle \mathbf{0} | L \exp(-T), \quad (\text{A3})$$

$$L = 1 + \Lambda, \quad (\text{A4})$$

and

$$|\Psi_{CC}\rangle = \exp(T) |\mathbf{0}\rangle. \quad (\text{A5})$$

Here T is the excitation operator that serves to parameterise the CC wavefunction, and Λ are the CC response amplitudes [55, 56]. $|\mathbf{0}\rangle$ is the reference wavefunction, taken here as the SCF solution.

Clearly the latter expression for the DBOC (Equation (A2)) is advantageous for evaluating this correction, as second derivatives of the wavefunction are expensive to calculate, whereas the former (Equation (A1)) better lends itself to analysis of the pole structure of the adiabatic correction, as it avoids derivatives of L . However, we shall start with Equation (A1), and then recast $\partial L / \partial \alpha$ in terms of commutators of \hat{H}_N and $\partial T / \partial \alpha$.

We begin with the form of the DBOC given by Gauss *et al.* [33],

$$\Delta E_{DBOC} = \sum_{\alpha}^{3N} \frac{1}{2M_{\alpha}} \left(\left\langle \frac{\partial}{\partial \alpha} \tilde{\Psi}_{CC} \left| \frac{\partial}{\partial \alpha} \Psi_{CC} \right\rangle + \left| \left\langle \tilde{\Psi}_{CC} \left| \frac{\partial}{\partial \alpha} \right| \Psi_{CC} \right\rangle \right|^2 \right). \quad (\text{A6})$$

Here, and in the rest of the derivation, terms involving derivatives of the reference wavefunction will be excluded, as they will not contribute to the correlation pole structure. Expanding the above equation, we get

$$\begin{aligned} \Delta E_{DBOC} &= \sum_{\alpha}^{3N} \frac{1}{2M_{\alpha}} \left(\langle \mathbf{0} | \frac{\partial}{\partial \alpha} (L \exp(-T)) \frac{\partial}{\partial \alpha} (\exp(T)) | \mathbf{0} \rangle \right. \\ &\quad \left. + \left| \langle \mathbf{0} | L \exp(-T) \frac{\partial}{\partial \alpha} (\exp(T)) | \mathbf{0} \rangle \right|^2 \right) \\ &= \sum_{\alpha}^{3N} \frac{1}{2M_{\alpha}} \left(\langle \mathbf{0} | \left(\frac{\partial L}{\partial \alpha} \exp(-T) - L \exp(-T) \frac{\partial T}{\partial \alpha} \right) \right. \\ &\quad \left. \times \exp(T) \frac{\partial T}{\partial \alpha} | \mathbf{0} \rangle \right. \\ &\quad \left. + \left| \langle \mathbf{0} | L \exp(-T) \exp(T) \frac{\partial T}{\partial \alpha} | \mathbf{0} \rangle \right|^2 \right) \\ &= \sum_{\alpha}^{3N} \frac{1}{2M_{\alpha}} \left(\langle \mathbf{0} | \frac{\partial L}{\partial \alpha} \frac{\partial T}{\partial \alpha} | \mathbf{0} \rangle - \langle \mathbf{0} | L \frac{\partial T}{\partial \alpha} \frac{\partial T}{\partial \alpha} | \mathbf{0} \rangle \right. \\ &\quad \left. + \left| \langle \mathbf{0} | L \frac{\partial T}{\partial \alpha} | \mathbf{0} \rangle \right|^2 \right). \quad (\text{A7}) \end{aligned}$$

First we address the leftmost term, A ,

$$A \equiv \langle \mathbf{0} | \frac{\partial L}{\partial \alpha} \frac{\partial T}{\partial \alpha} | \mathbf{0} \rangle. \quad (\text{A8})$$

Insert the identity, and the form of $\partial L/\partial\alpha$ given in part B of the appendix.

$$\begin{aligned} A &= \langle \mathbf{0} | \frac{\partial L}{\partial\alpha} | \mathbf{p} \rangle \langle \mathbf{p} | \frac{\partial T}{\partial\alpha} | \mathbf{0} \rangle \\ &= \left(-\langle \mathbf{0} | L \bar{H}_N \frac{\partial T}{\partial\alpha} | \mathbf{p} \rangle + \langle \mathbf{0} | L \frac{\partial T}{\partial\alpha} \bar{H}_N | \mathbf{p} \rangle - \langle \mathbf{0} | L \bar{H}_N^\alpha | \mathbf{p} \rangle \right) \\ &\quad \times \langle \mathbf{p} | \bar{H}_N | \mathbf{p} \rangle^{-1} \langle \mathbf{p} | \frac{\partial T}{\partial\alpha} | \mathbf{0} \rangle, \end{aligned} \quad (\text{A9})$$

where

$$\bar{H}_N \equiv \bar{H} - \langle \mathbf{0} | H | \mathbf{0} \rangle, \quad (\text{A10})$$

and

$$\bar{H}^\alpha \equiv \exp(-T) \frac{\partial H}{\partial\alpha} \exp(T). \quad (\text{A11})$$

It is convenient to partition the space of Slater determinants as follows: $\mathbf{0}$, which is the reference Slater determinant; \mathbf{g} , the determinants reached by operation of T onto the reference; \mathbf{p} , the union of $\mathbf{0}$ and \mathbf{g} ; and \mathbf{q} , the determinants outside the scope of the truncated CC treatment in question.

With this, the first term of A (I) can be separated into two contributions:

$$\begin{aligned} \text{I} &\equiv -\langle \mathbf{0} | L \bar{H}_N \frac{\partial T}{\partial\alpha} | \mathbf{p} \rangle \langle \mathbf{p} | \bar{H}_N | \mathbf{p} \rangle^{-1} \langle \mathbf{p} | \frac{\partial T}{\partial\alpha} | \mathbf{0} \rangle \\ &= \left(-\langle \mathbf{0} | L \bar{H}_N | \mathbf{p} \rangle \langle \mathbf{p} | \frac{\partial T}{\partial\alpha} | \mathbf{p} \rangle - \langle \mathbf{0} | L \bar{H}_N | \mathbf{q} \rangle \langle \mathbf{q} | \frac{\partial T}{\partial\alpha} | \mathbf{p} \rangle \right) \\ &\quad \times \langle \mathbf{p} | \bar{H}_N | \mathbf{p} \rangle^{-1} \langle \mathbf{p} | \frac{\partial T}{\partial\alpha} | \mathbf{0} \rangle. \end{aligned} \quad (\text{A12})$$

The first of these vanishes because $\langle \mathbf{0} | L \bar{H}_N | \mathbf{p} \rangle = 0$ (the defining equation of L), leaving only

$$\text{I} = -\langle \mathbf{0} | L \bar{H}_N | \mathbf{q} \rangle \langle \mathbf{q} | \frac{\partial T}{\partial\alpha} | \mathbf{p} \rangle \langle \mathbf{p} | \bar{H}_N | \mathbf{p} \rangle^{-1} \langle \mathbf{p} | \frac{\partial T}{\partial\alpha} | \mathbf{0} \rangle, \quad (\text{A13})$$

which includes the influence of excitations outside the range defined by the truncated level of theory (for instance, triples, quadruples, etc, for CCSD).

The second term of A (II) simplifies to

$$\begin{aligned} \text{II} &\equiv \langle \mathbf{0} | L \frac{\partial T}{\partial\alpha} \bar{H}_N | \mathbf{p} \rangle \langle \mathbf{p} | \bar{H}_N | \mathbf{p} \rangle^{-1} \langle \mathbf{p} | \frac{\partial T}{\partial\alpha} | \mathbf{0} \rangle \\ &= \langle \mathbf{0} | L \frac{\partial T}{\partial\alpha} | \mathbf{p} \rangle \langle \mathbf{p} | \bar{H}_N | \mathbf{p} \rangle \langle \mathbf{p} | \bar{H}_N | \mathbf{p} \rangle^{-1} \langle \mathbf{p} | \frac{\partial T}{\partial\alpha} | \mathbf{0} \rangle \\ &= \langle \mathbf{0} | L \frac{\partial T}{\partial\alpha} \frac{\partial T}{\partial\alpha} | \mathbf{0} \rangle, \end{aligned} \quad (\text{A14})$$

which cancels the second term of Equation (A7). Gathering all of the terms of Equation (A7) yields the easily analyzed form:

$$\begin{aligned} \Delta E_{\text{DBOC}} &= \sum_{\alpha} \frac{3N}{2M_{\alpha}} \left(-\langle \mathbf{0} | L \bar{H}_N | \mathbf{q} \rangle \langle \mathbf{q} | \frac{\partial T}{\partial\alpha} | \mathbf{p} \rangle \langle \mathbf{p} | \bar{H}_N | \mathbf{p} \rangle^{-1} \right. \\ &\quad \times \langle \mathbf{p} | \frac{\partial T}{\partial\alpha} | \mathbf{0} \rangle - \langle \mathbf{0} | L \bar{H}_N^\alpha | \mathbf{p} \rangle \langle \mathbf{p} | \bar{H}_N | \mathbf{p} \rangle^{-1} \langle \mathbf{p} | \frac{\partial T}{\partial\alpha} | \mathbf{0} \rangle \\ &\quad \left. + \left| \langle \mathbf{0} | L \frac{\partial T}{\partial\alpha} | \mathbf{0} \rangle \right|^2 \right). \end{aligned} \quad (\text{A15})$$

Short of full CI, the CC level DBOC clearly displays a complicated pole structure, with the first term (which makes a third-order contribution) in the equation above dominating close to the crossing of the states (see similar, but more detailed, analysis in ref. [41]). At full CI this leading term vanishes and ‘proper’ (second order) behaviour is regained. Additionally, at full CI, the sign of the DBOC is necessarily positive, as is demanded on physical grounds from the expectation value of the kinetic energy.

A.2 Deriving $\partial L/\partial\alpha$

In the above text, a useful substitution was made that expressed $\partial L/\partial\alpha$ in terms of commutators of $\partial T/\partial\alpha$ and \bar{H}_N , which is shown below.

We begin with the defining equation for the L operator.

$$\langle \mathbf{0} | L \bar{H}_N | \mathbf{p} \rangle = 0. \quad (\text{A16})$$

The derivative of which is

$$\begin{aligned} \langle \mathbf{0} | \frac{\partial L}{\partial\alpha} \bar{H}_N | \mathbf{p} \rangle + \langle \mathbf{0} | L \bar{H}_N \frac{\partial T}{\partial\alpha} | \mathbf{p} \rangle \\ - \langle \mathbf{0} | L \frac{\partial T}{\partial\alpha} \bar{H}_N | \mathbf{p} \rangle + \langle \mathbf{0} | L \bar{H}_N^\alpha | \mathbf{p} \rangle = 0. \end{aligned} \quad (\text{A17})$$

Then,

$$\begin{aligned} \langle \mathbf{0} | \frac{\partial L}{\partial\alpha} | \mathbf{p} \rangle &= \left(-\langle \mathbf{0} | L \bar{H}_N \frac{\partial T}{\partial\alpha} | \mathbf{p} \rangle + \langle \mathbf{0} | L \frac{\partial T}{\partial\alpha} \bar{H}_N | \mathbf{p} \rangle \right. \\ &\quad \left. - \langle \mathbf{0} | L \bar{H}_N^\alpha | \mathbf{p} \rangle \right) \langle \mathbf{p} | \bar{H}_N | \mathbf{p} \rangle^{-1}, \end{aligned} \quad (\text{A18})$$

which is used above.